Available online at www.sciencedirect.com
ScienceDirect
Materials and Design 28 (2007) 797–803
Materials & Design
www.elsevier.com/locate/matdes

The effect of matrix structure on the fatigue behavior of austempered ductile iron

M. Tayanç [a], K. Aztekin [b], A. Bayram [c,*]

[a] Balikesir University, Faculty of Engineering and Architecture, Çağış, 10145 Balikesir, Turkey
[b] Land Forces NCO, Vocational School of Higher Education, Çayırhisar, 10050 Balikesir, Turkey
[c] Uludağ University, Faculty of Engineering and Architecture, Görükle, 16059 Bursa, Turkey

Received 12 May 2005; accepted 17 November 2005
Available online 19 January 2006

Abstract

The primary objective of this study has been to investigate the fatigue behavior of the austempered unalloyed ductile iron. Ductile iron specimens were austenized at 900 °C for 110 min and then one group specimens were austempered at 230, 330, 430 °C for 60 min, and another one group specimens were austempered at 330 °C for 30, 60, 120 min to obtain different microstructures. Rotating bending tests (10 million cycles) were conducted on the ductile iron and the austempered specimens selecting completely reversed cycle of stress (R = minimum stress/maximum stress = −1). The highest fatigue strength was found in the bainitic structure (ausferritic). The presence of martensite or carbide phases in the structure of austempered ductile iron reduces the fatigue strength.

Keywords: Casting C.; Heat treatment C.; Fatigue E.; Microstructure F.

1. Introduction

Austempered ductile iron (ADI) has attracted considerable interest in recent years because of its excellent mechanical properties such as high strength together with good ductility, good wear resistance, and good fatigue properties. The remarkable properties of ADI are attributed to its unique microstructure consisting of high carbon austenite and ferrite [1]. This structure is known as bainitic matrix. Bainitic structure in ductile iron can be obtained in two ways: (i) In the as-cast form where bainitic transformation is achieved by alloying elements such as Ni, Mo, and Cr and (ii) by subjecting conventional ductile iron castings to a specific heat treatment known as austempering [2].

Recent studies [3–7] have shown that this new family of engineering materials also offers great potential for cast parts in application involving many critical components in automobiles, such as crank shafts, steering knuckles and hypoid rear axle gear. The application of these irons is expected to increase in the future, not only in the automobile industry, but also in many other fields such as cast iron parts in application involving impact loads combined with wear, rail, and heavy engineering industry.

The fatigue properties of ductile iron and ADI have been studied by many researchers. Marrow and Çetinel [8] investigated the growth of short fatigue cracks in ADI. It was proposed that the arrest and retardation of short crack nuclei was controlled by the austenite grain size and graphite nodule size. Kim and Kim [9] also examined influence of microstructure on fatigue limits of high strength ductile irons applying rotary bending fatigue test. Their result showed that in case of series B (bainite) the fatigue limit was higher than in case of series A (sorbite) and fatigue limits of series A, and B were improved compared with as cast specimens.

Bartosiewicz et al. [10] studied the effect microstructure on high-cycle fatigue properties of ADI. The results of this investigation demonstrated that the fatigue threshold of the

* Corresponding author. Tel.: +90 224 4428174; fax: +90 224 4428021.
E-mail address: bayram@uludag.edu.tr (A. Bayram).

0261-3069/$ - see front matter © 2005 Elsevier Ltd. All rights reserved.
doi:10.1016/j.matdes.2005.11.010

material increased with the increase in volume fraction of carbon-saturated austenite. The fatigue strength of the material was found to increase with the decrease in austenite grain size. Lin et al. [11] performed another study which was about the effect of microstructure on fatigue properties of these materials. It was found that the mechanical properties and high cycle fatigue strength of ductile irons could be markedly improved by austempering heat treatment and the high cycle fatigue strength of ADI was increase with increasing nodularity and nodule count.

Lin and Lee [12] exhibited the relationship between fatigue strength and highly stressed volume with various combinations of specimen configurations and loading modes for ADI. Lin and Fu [13] also investigated the relationship between low-cycle fatigue strength of ADI and cast section size and location. Luo et al. [14] determined fatigue behavior for ferritic, pearlitic irons, and ADI under tension–tension loading.

Bahmani and Elliott [15] showed the relationship between fatigue strength and microstructure in ADI. The correlation between fatigue strength and austempered microstructure was evaluated depending on the amount of high austenite, Xγ, and its carbon content, Cγ. They observed that fatigue strength increased as Xγ, and Cγ increased. Thomson et al. [16] aimed to develop a generic model that will enable the producers of ADI to optimize their product in terms of microstructure and mechanical properties.

Jen et al. [17] determined fatigue properties of ductile iron which were applied on four different grades austempered heat treatment under bending fatigue test. They observed that the estimated endurance limits were mainly depended on the hardness of the ADI. Krishnaranj et al. [18] investigated fatigue behavior of ductile iron with different matrix structures. It was reported that among ductile iron with different matrix structures, the one with bainitic matrix possessed the highest fatigue limit.

In this present work, unalloyed ductile iron was austempered at different temperatures and times. Following this, fatigue properties of ductile iron and ADI were examined under rotating bending tests. Besides, the microstructural and fractography features of these materials were investigated using optical and scanning electron microscopy.

2. Experimental techniques and methods

The ductile iron used in this study was of composition 3.90 wt% C, 2.10 wt% Si, 0.063 wt% Mn, 0.022 wt% Mg, 0.018 wt% Ni, 0.025 wt% P, 0.011 wt% S, balance is iron. Ductile iron was poured in keel block molds (Fig. 1). All the specimens were taken from the legs of keel block in order to avoid structural defects.

In order to investigate the effect of bainitic structure (ausferitic) on fatigue behavior, different austempering treatment was applied to selected ductile iron. Austempering heat treatment cycle consists of austenitizing, quenching, austempering, and air-cooling. All the test specimens were austenized at 900 °C for 110 min and then I group specimens were austempered at 230, 330, 430 °C for 60 min, respectively, A1, A2, A3, II. Group specimens was austempered at 330 °C for 30, 60, 120 min, respectively, A4, A2, A5. Austempering heat treatment was carried out in a salt bath.

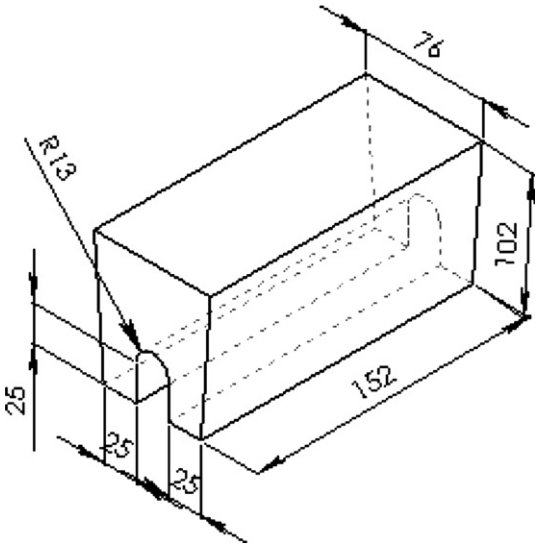

Fig. 1. Geometry of keel block.

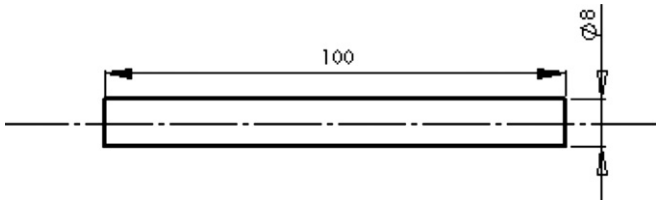

Fig. 2. Dimensions of fatigue test specimen.

Optical micrographs of cast iron and austempered samples were taken on an Olympous metal microscope etching with %5 nital after grinding and polishing. Fracture surfaces of the specimens were examined under scanning electron microscope (SEM).

Fatigue tests were accomplished with a rotating beam machine. Rotating bending tests were performed at a frequency of 50 Hz (2950 rpm) for each specimen. It was selected completely reversed cycle of stress (R = minimum stress/maximum stress = −1) in fatigue tests. The fatigue test specimens used in the present work are depicted in Fig. 2. Twelve samples were tested at each stress level and a sufficient number of stress levels were chosen to obtain S–N curves of each heat treatment condition. The highest stress at which the samples endured 10^7 cycles was taken as the fatigue strength.

The bending stress was calculated using the following equation

$$\sigma_g = \frac{M_{e\max}}{W} = \frac{PI}{\pi d^3/32} = \frac{PI32}{\pi d^3}, \quad (1)$$

where σ_g is the stress amplitude, $M_{e\max}$ is maximum bending moment (N m), W is section modulus (mm^3), P is applied load (N), I is moment of length (80 mm), and d is the diameter of test sample (d = 8 mm).

3. Results and discussion

3.1. Metallography

Fig. 3 reveals the micrograph of cast-ductile iron. The cast structure is of typical bull's-eye type with surrounding

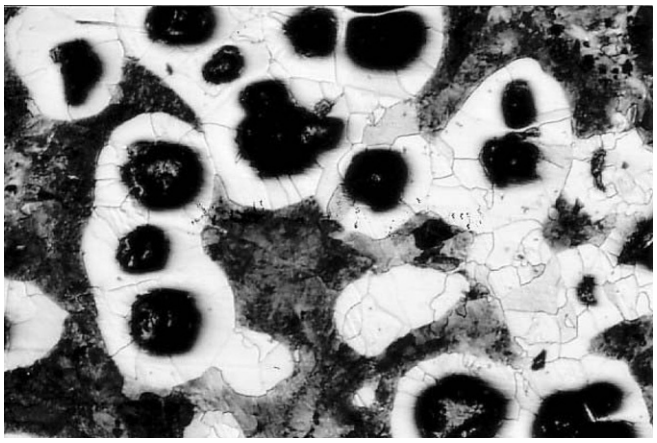

Fig. 3. Microstructure of cast-ductile iron (50×).

the graphite nodules in pearlite matrix. Fig. 4a–e show the micrographs of austempered ductile iron at different heat treatment condition. As shown in Fig. 4a, A2 exhibits martensitic structure with lath martensitic packets. However, this figure also shows bainite islets. This micrograph exhibits that the stage I reaction is not completed. At higher austempering temperatures, which are used to achieve the high ductility grades of the standard, the stage I reaction transforms the low carbon into bainitic ferrite and high carbon austenite (ausferritic structure) [19].

As can be seen Fig. 4b, bainite structure and retained austenite was observed in A4. This can be explained by taking into account that, for short time, the transformation to bainite is not completed. It is apparent that bainitic (ausferritic) structure from Fig. 4c,d, however specimen austempered

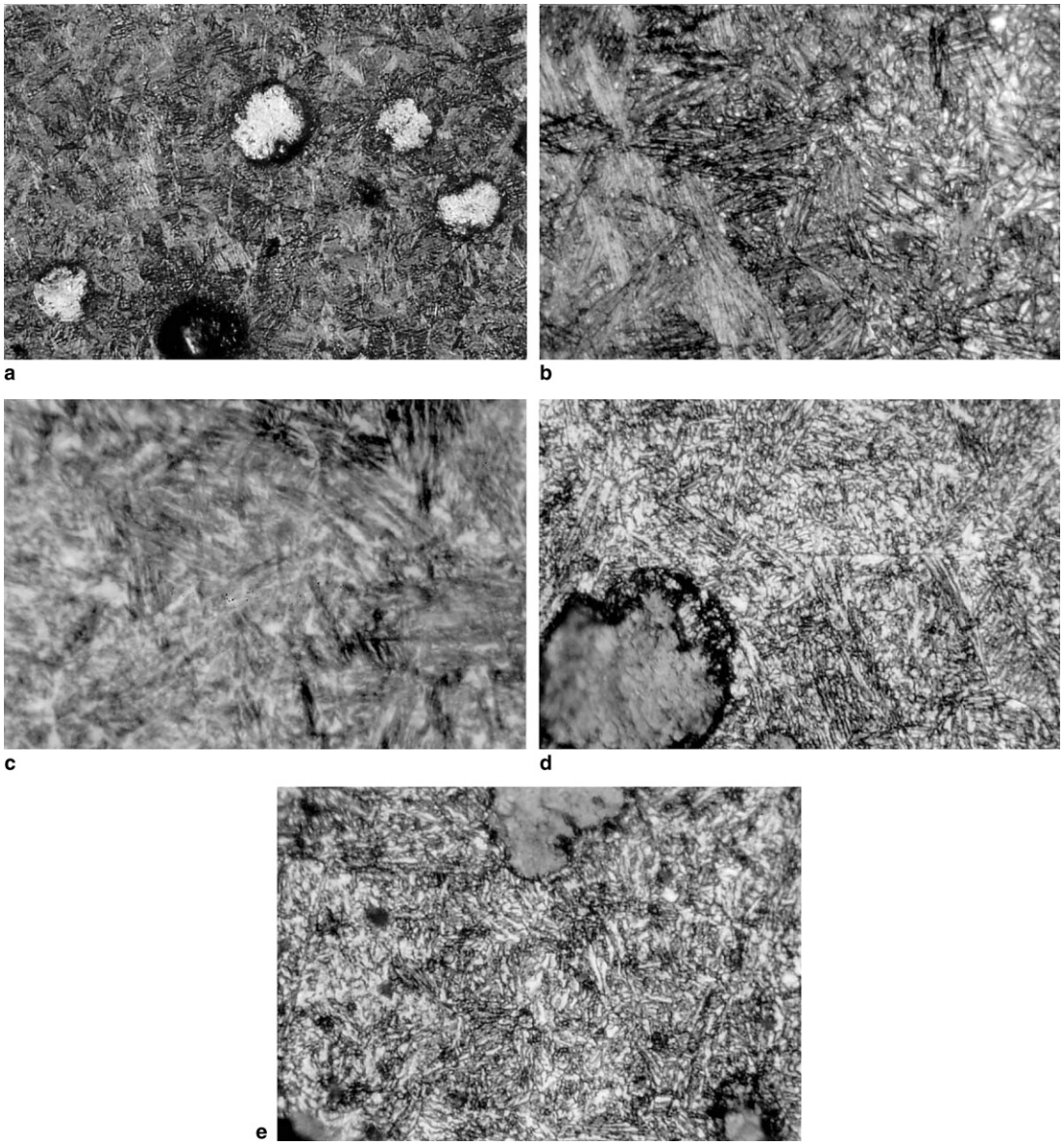

Fig. 4. (a) Microstructure of austempered sample at 230 °C for 60 min (100×), (b) Microstructure of austempered sample at 330 °C for 30 min (400×), (c) Microstructure of austempered sample at 330 °C for 60 min (400×), (d) Microstructure of austempered sample at 330 °C for 120 min (400×) and (e) Microstructure of austempered sample at 430 °C for 60 min (400×).

for 120 min, exhibits a little ferrite and carbide. When comparing the microstructures for different austempering times at 330 °C, it is clear that the sample austempered for 60 min showed feathery-type ferrite characteristics of bainitic microstructure and while those austempered for 30 and 120 min showed acicular ferrite characteristics of bainitie, respectively, Fig. 4c,d. Since diffusion of carbon depends on time and temperature, the diffusion of carbon from regions transforming into ferrite to the surrounding austenite is short than that of longer time at short austempering time [1]. Consequently, ferrite needles are finer at short austempering time (30 min).

A3 did not exhibit ausferritic structure. This sample reveals that the high carbon austenite breaks down into ferrite and carbide (Fig. 4e). In other words, the stage II reaction has occurred. As the austempering temperature increases the window narrows and can be closed at the highest austempering and austenitising temperatures [1]. Therefore, the narrow window takes to the stage II reaction.

3.2. Fatigue behavior

The *S–N* curves of the rotary bending fatigue tests are depicted in Figs. 5–10. The *S–N* curves are drawn through the data points as best fit lines. In each figure, data points with arrows indicate samples that did not fail after an excess of 10^7 cycles or more stress cycle.

Fig. 5 represents the fatigue results obtained from the as-cast ductile iron. Fatigue strength at 10^7 cycles was found to be 233 MPa. Similar result is also reported in the literature [18]. Figs. 6–10 summarize the fatigue results of ADI at different temperature and times. The highest fatigue strength was achieved at austempered specimens in A2. A1 exhibited the lowest fatigue strength.

It was observed that the fatigue strength increased as the temperature increased from 230 to 330 °C. However, the fatigue strength decreased with increasing temperature

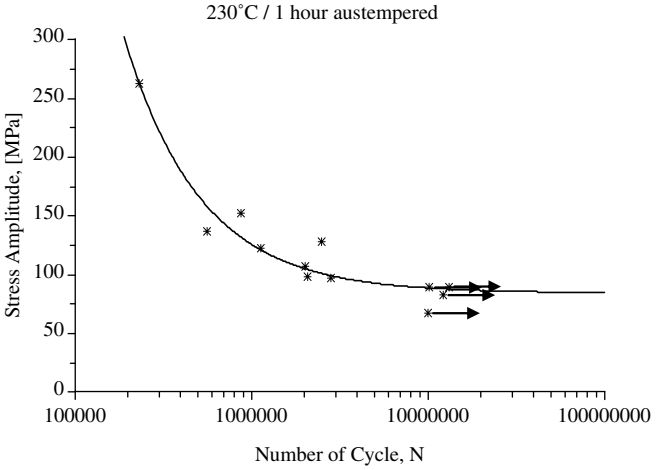

Fig. 6. *S–N* curve of austempered samples at 230 °C for 60 min. Arrows show that the samples did not fail in excess of 10^7 cycles.

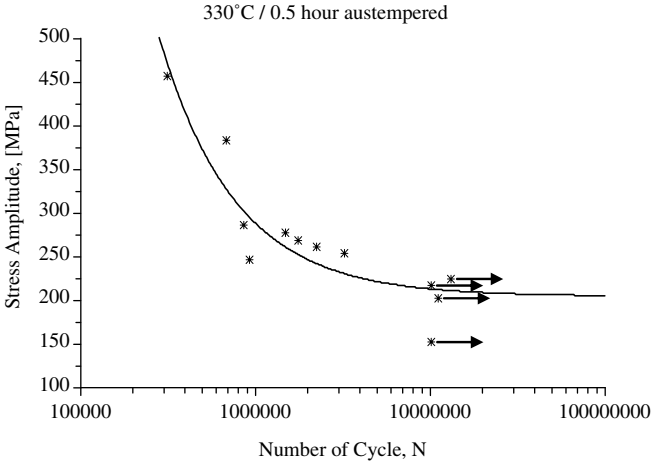

Fig. 7. *S–N* curve of austempered samples at 330 °C for 30 min. Arrows show that the samples did not fail in excess of 10^7 cycles.

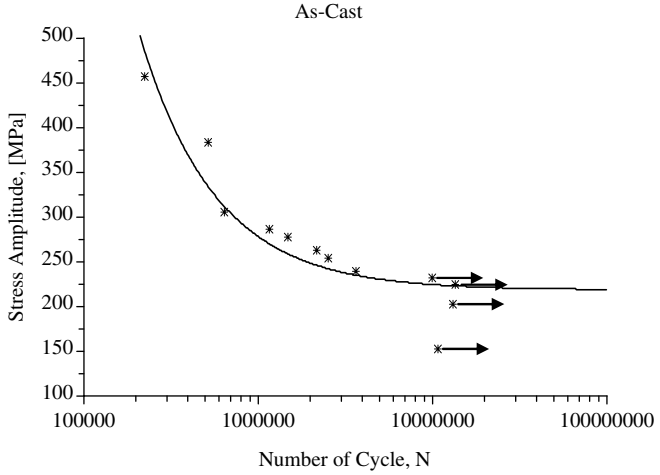

Fig. 5. *S–N* curve of cast-ductile iron. Arrows show that the samples did not fail in excess of 10^7 cycles.

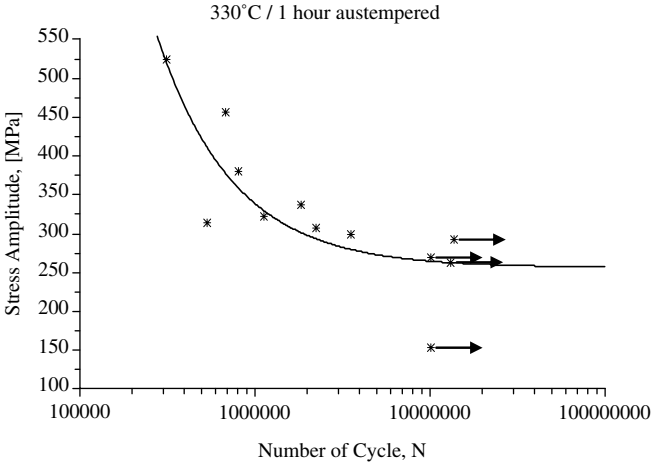

Fig. 8. *S–N* curve of austempered samples at 330 °C for 60 min. Arrows show that the samples did not fail in excess of 10^7 cycles.

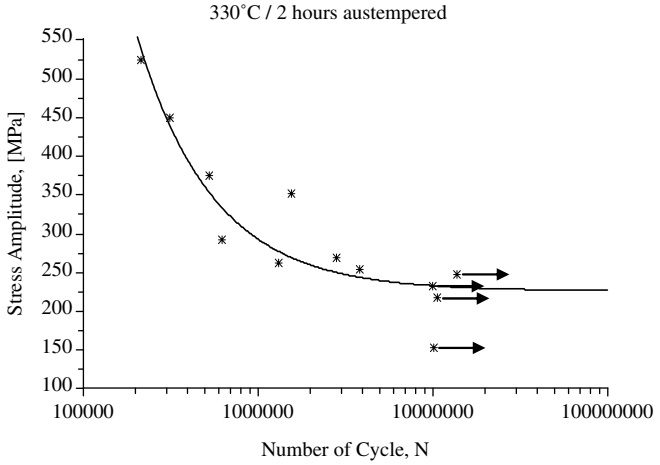

Fig. 9. *S–N* curve of austempered samples at 330 °C for 120 min. Arrows show that the samples did not fail in excess of 10^7 cycles.

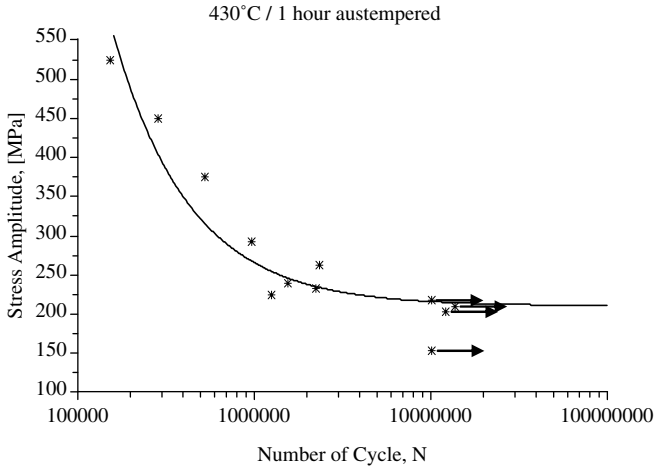

Fig. 10. *S–N* curve of austempered samples at 430 °C for 60 min. Arrows show that the samples did not fail in excess of 10^7 cycles.

from 330 to 430 °C (Table 1). These results found in this present work are consistent with the literature. The fatigue strength reaches the highest value with austempering at temperatures around 360 °C and when austempered at the higher temperatures from 360 to 430 °C, the fatigue strength decreases [11,12,15].

The reason why the fatigue strengths of DI with austempering temperature show difference might be explained by the carbon content of austenite. The resistance to crack propagation and the fatigue strength would be expected to depend on the amount and nature of the high C austenite and the fineness of austempered structure. Bahmani et al. [15] determined that fatigue strength increased at each of the austenitising temperatures as the austempering time at 370 °C increases from 30 to 120 min This corresponds to a reduction in the amount of unreacted low C austenite in the austempered structure. Because, it is known that low C austenite is thermally unstable and transforms to martensite that lead to reducing the resistance to crack growth and fatigue strength [15]. The austempering at higher temperature from 360 °C starts stage II reaction, so that the carbide precipitates at ferrite–austenite phase boundaries cause a reduction in the fatigue limits.

Table 1
The fatigue strength of the cast-ductile iron and austempered ductile irons

Austemperig heat treatment	Fatigue strength (MPa)
Cast-ductile iron	233
230 °C for 60 min	90
330 °C for 30 min	225
330 °C for 60 min	293
330 °C for 120 min	248
430 °C for 60 min	218

High austempering temperature results in coarse microstructure with a fairly large amount of austenite. Reducing the austempering temperature favors the formation of finer microstructure. Because a lower austempering temperature results in a large undercooling of the austenite and slow diffusion rate of carbon, the nucleation of ferrite plates rather than their growth is favored, resulting in a finer structure [5].

On the other hand, it was determined that the fatigue strength increased while austempering time increased from 30 to 60 min at 330 °C, however the fatigue strength decreased with increasing time from 60 to 120 min at 330 °C (Table 1). As mentioned above, this behavior could also be explained by the carbon content of austenite.

3.3. Fractography

SEM micrographs of the fracture surfaces of fatigued specimens are shown in Fig. 11a–e. It can be seen that the cast-ductile iron specimen reveals generally ductile fracture dimple formation together with some cleavage fracture (Fig. 11a). As shown in Fig. 11b, fracture surface of A1 exhibited brittle cleavage type. The fracture of A2 is entirely ductile (Fig. 11c). A3 shows almost cleavage fracture (Fig. 11d).

Fracture observations support the experimental results. Thus, A2, with the highest fatigue strength values, fractures in completely ductile mode. Cast-ductile iron has lower fatigue strength values but exhibits a mostly ductile fracture. A1, with the lowest fatigue strength values, displays mostly brittle cleavage cracking.

Previous studies [11,13,15,20] have shown that fatigue cracks initiate at the interface between graphite nodules, and the matrix or from casting imperfections such as inclusions, large microshrinkage pores and irregularly shaped graphite. The fatigue crack follows the path of least resistance through the matrix between nodules [15]. As have been observed by Bahmani et al. [15], Fig. 11e exhibits crack initiation at the nodule matrix interface at the intercellular boundaries and crack path through the path of least resistance at the intercellular boundary after nucleation a pore. Fatigue crack was observed to grow along the austenite/ferrite interfaces or cut through the lath of austenite and ferrite, which was also reported by Voigt [20].

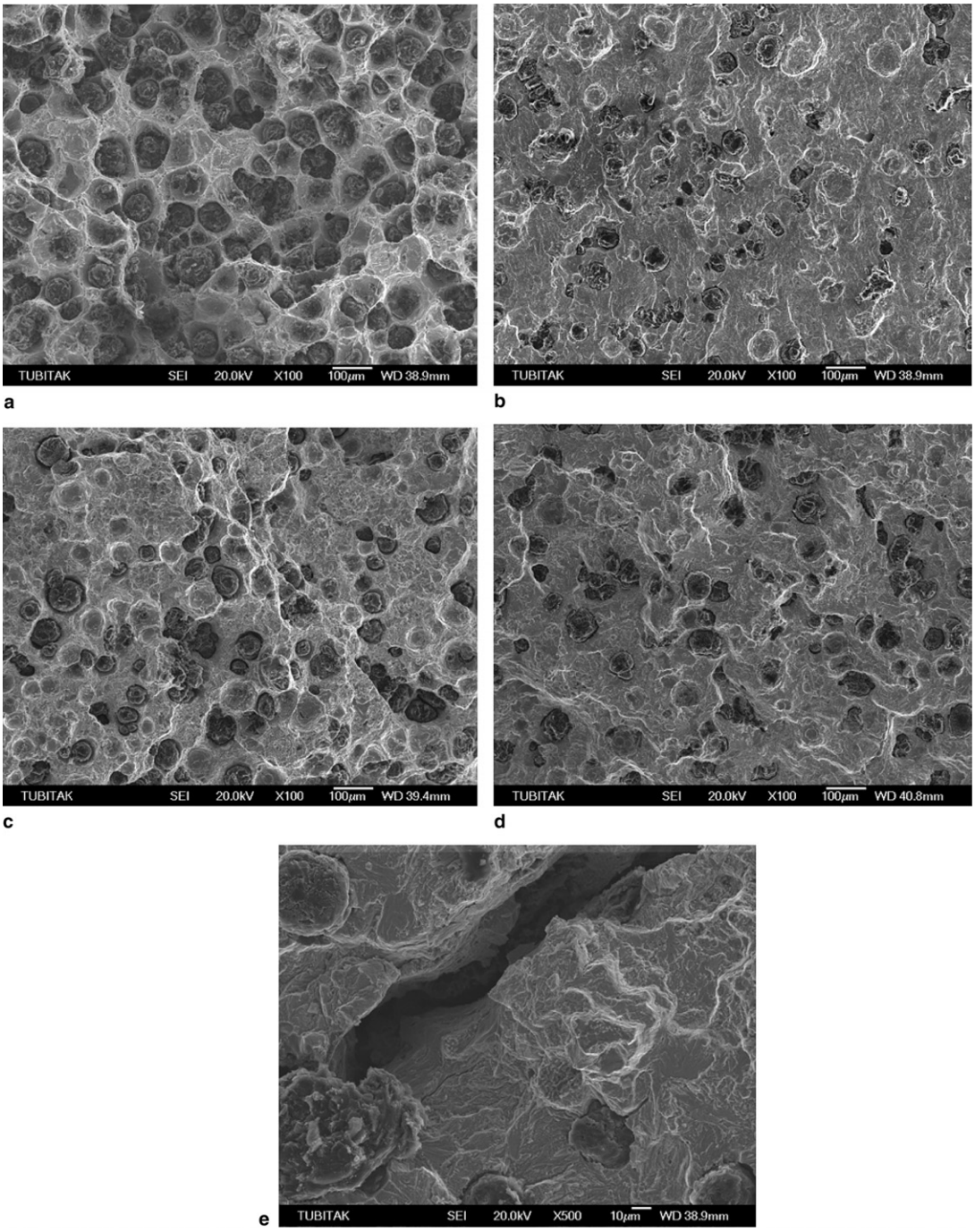

Fig. 11. (a) SEM fractographs of cast-ductile iron fatigue specimen. (b) SEM fractographs of austempered fatigue specimen at 230 °C for 60 min. (c) SEM fractographs of austempered fatigue specimen at 330 °C for 60 min. (d) SEM fractographs of austempered fatigue specimen at 430 °C for 60 min and (e) SEM fractographs of austempered fatigue specimen at 330 °C for 60 min.

4. Conclusion

The fatigue strength of ductile iron could be improved by austempering heat treatment, except austempering at 230 °C. Feathery-type ferrite characteristics of bainitic microstructure result in higher fatigue strength than acicular ferrite characteristics of bainitic microstructure. Carbide precipitation takes place in loss of fatigue strength. However, specimen with martensite matrix austempered at 230 °C shows the lowest fatigue strength.

References

[1] Putatunda SK, Gadicherla K. Effect of austempering time on mechanical properties of a low manganese austempered ductile iron. J Mater Eng Perform 2000;9(2):193–203.

[2] Refaey A, Fatahalla N. Effect of microstructure on properties of ADI and low alloyed ductile iron. J Mater Sci 2003;38:351–62.
[3] Shanmugam P, Rao PP, Udupa N, Venkataraman N. Effect of microstructure on the fatigue strength of an austempered ductile iron. J Mater Sci 1994;29:4933–40.
[4] Lerner YS, Kingsbury GR. Wear resistance properties of austempered ductile iron. J Mater Eng Perform 1998;7(1):48–52.
[5] Trudel A, Gagne M. Effect of composition and heat treatment parameters on the characteristics of austempered ductile irons. Can Metall Quart 1997;36(5):289–98.
[6] Bosnjak B, Radulovic B, Pop-Toner K, Asanovic V. Influence of microalloying and heat treatment on the kinetics of bainitic reaction in austempered ductile iron. J Mater Eng Perform 2001;10(2): 203–11.
[7] Dai PQ, He ZR, Zheng CM, Mao ZY. In situ SEM observation on the fracture of austempered ductile iron. Mater Sci Eng A 2001;319–321:531–4.
[8] Marrow TJ, Çetinel H. Short fatigue cracks in austempered ductile cast iron. Fatigue Fract Eng Mater Struct 2000;23:425–34.
[9] Kim JH, Kim MG. Influence of microstructure on fatigue limit of high strength ductile irons. Key Eng Mater 2000;183–187: 933–8.
[10] Bartosiewicz L, Krause AR, Alberts FA, Singh I, Patunda SK. Influence of microstructure on high-cycle fatigue behavior of austempered cast iron. Mater Charact 1993;30:221–34.
[11] Lin CK, Lai PK, Shih TS. Influence of microstructure on the fatigue properties of austempered ductile irons-I. High-cycle fatigue. Int J Fatigue 1996;18:297–307.
[12] Lin CK, Lee WJ. Effect of highly stressed volume on fatigue strength of austempered ductile irons. Int J Fatigue 1998;20:301–7.
[13] Lin CK, Fu CS. Low-cycle fatigue of austempered ductile irons in various-sized Y-block casting. Mater Trans JIM 1997;38:692–700.
[14] Luo J, Harding RA, Bowen P. Evaluation of the fatigue behavior of ductile irons with various matrix microstructures. Metall Mater Trans A 2002;33A:3719–29.
[15] Bahmani M, Elliot R, Varahram N. The relationship between fatigue strength and microstructure in an austempered Cu–Ni–Mn–Mo alloyed ductile iron. J Mater Sci 1997;32:5383–8.
[16] Thomson RC, James JS, Putman DC. Modelling microstructural evolution and mechanical properties of austempered ductile iron. Mater Sci Technol 2000;16:1412–9.
[17] Jen KP, Kim S. Study of fracture and fatigue behavior of austempered ductile iron. AFS Trans 1992;92:92–133.
[18] Krishnaraj D, Rao KV, Seshan S. Influence of matrix structure on the fatigue behavior of ductile iron. AFS Trans 1989;97:315–20.
[19] Nazarboland A, Alliot R. Influence of heat treatment parameters on stepped austempering of 0.37%Mn–Mo–Cu ductile iron. Mater Sci Technol 1997;13:223–32.
[20] Voigt RC. Microstructural analysis of austempered ductile iron using the scanning electron microscope. AFS Trans 1983;91:253–62.